MODELING AND CONTROL OF A POWERED WHEELCHAIR: WALL-FOLLOWING AROUND A CORNER WITH INFRARED

Meeko Oishi*, **Pouyan TaghipourBibalan**†, **Alexis Cheng**†
Electrical and Computer Engineering
University of British Columbia, Vancouver, BC, Canada
***moishi@ece.ubc.ca**
†**pbibalan, akcheng@interchange.ubc.ca**

Ian Mitchell‡
Computer Science
University of British Columbia
Vancouver, BC, Canada
‡**mitchell@cs.ubc.ca**

ABSTRACT

Smart wheelchairs will play an increasing role in enabling mobility in older adults. We describe the modeling and feedback linearizing control of an autonomous powered wheelchair for wall following around a corner, one of the many skills required for safe operation of human-controlled power wheelchairs. The controller is implemented on an experimental testbed, with only an infrared sensor and wheel encoders for feedback, by using an extended Kalman filter to obtain an accurate state estimate. Our results indicate high performance despite noisy measurements.

INTRODUCTION

For people with significant movement impairments (from stroke, Parkinson's disease, cerebral palsy, and others) manually-operated wheelchairs can be extremely difficult, if not impossible, to use. Smart wheelchairs have the potential to improve mobility and independence for tens of thousands of Canadians [1], [2], [3], particularly amongst older adults with severe physical or cognitive disabilities. However, for the approximately 200,000 seniors with disabilities who reside in long-term care facilities [4], powered wheelchairs are often not prescribed because of the danger that these large, powerful machines pose to the operator, residents, staff, and the facility.

Driving conditions are a significant factor in many accidents involving powered wheelchairs [5]. Powered mobility users must navigate precisely around fixed obstacles (e.g., carts, custodial equipment) in narrow hallways, through narrow doorways, and around tight corners. In addition, powered mobility users face moving obstacles which include other wheelchair users and walkers, each traveling at a wide range of speeds. Smart wheelchairs that can reduce or even eliminate collisions or near-collisions with fixed and mobile obstacles in the environment have the potential to reduce the liability associated with powered wheelchairs in residential care facilities. CanWheel, a newly formed collaboration based at the University of British Columbia, is focused on the design, implementation, and basic user testing of a modular, robust, and safe smart wheelchair for older adults.

A number of smart wheelchairs have been designed, built, and tested since the early 1990s [6]. Collision prevention schemes [7], [8] have been developed to stop the chair upon detection of a collision via bumper skirt [9] or via laser range finders or stereovision cameras that detect an obstacle within a certain distance of the chair [10]. Some chairs provide vocal prompts to the user [7], [11] after the stop, or attempt to guide the user to another heading or path [12], [13]. The SmartWheeler chair interprets voice commands from the user [14]. Related work in wheeled mobile robots has employed sonar to autonomously follow a straight wall [15], [16].

We describe in this paper the modeling and control of a powered wheelchair with integrated IR, sonar, and bumperskirt for autonomous navigation implemented in ROS [17], an open-source operating system tailored to reconfigurable robotic systems, under a Controller Area Network (CANBus) communication framework. Using only infrared rangefinders and wheel encoders, we demonstrate the system for wall following around a corner, a moderately difficult task from the Powered Wheelchair Skills Test [18]. Although designed for human operators of powered wheelchairs, the Powered Wheelchair Skills Test provides a good benchmark for performance of autonomous wheelchairs [14], as it represents a set of skills necessary for safe navigation through real-world hazards.

MODELING

We model the planar motion of the wheelchair (Figure 1) by a kinematic model with inertial state $x = [x, y, \theta]$ [19] (with slight abuse of notation).

$$\begin{aligned} \dot{x} &= V\cos\theta \\ \dot{y} &= V\sin\theta \\ \dot{\theta} &= \omega \end{aligned} \tag{1}$$

The wheelchair travels with velocity $V = \frac{r}{2}(\Omega_r + \Omega_l)$, turn rate $\omega = \frac{r}{W}(\Omega_r - \Omega_l)$, and has wheel radius r and distance W between the wheels. The inputs Ω_r, Ω_l are angular velocities of the right and left wheels, respectively.

We consider the general problem of following a wall at angle γ and at a distance R from the inertial coordinate system, as shown in Figure 2. The distance to the wall measured by the infrared sensor is

$$d_{\mathrm{IR}}(x) = \frac{x_s\cos\gamma + y_s\sin\gamma - R}{\cos(\alpha_s - \gamma)} \tag{2}$$

where the position of the sensor $[x_s, y_s] = \mathrm{Rot}(\theta)[x, y]$ is a fixed distance $[x'_s, y'_s]$ from the wheelchair center of rotation,

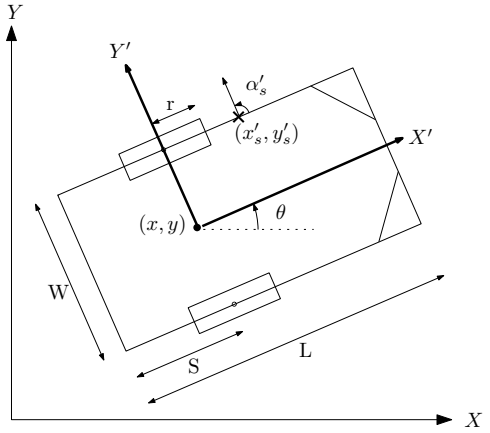

Fig. 1. Planar configuration of a powered wheelchair.

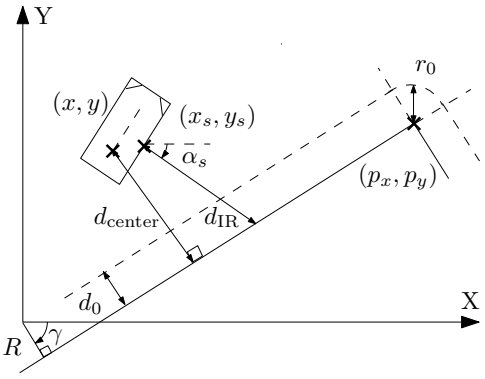

Fig. 2. Geometry of wall following around a corner.

as shown in Figure 1, and $\alpha_s = \theta + \alpha'_s$. The distance to the wall from the center of rotation is

$$d_{\text{center}}(x) = x\cos\gamma + y\sin\gamma - R \tag{3}$$

For our powered wheelchair, $L = 140$cm, $W = 60$cm, $r = 18$cm, $S = 50$cm, $x'_s = 0$cm, $y'_s = 30$cm, $\alpha'_s = 90°$.

WALL-FOLLOWING CONTROL

Two controllers have been designed: one for maintaining a distance d_0 from the wall, and one for turning around a corner at a constant radius r_0. In both cases, the wheelchair travels at a constant speed $V = 0.1$m/s.

A. Wall Following

We use input-output linearization (1) with input ω since the map $[V, \omega] \to [\Omega_r, \Omega_l]$ is smooth and invertible. The output is the distance from the center of rotation to the wall (3). With the appropriate Lie derivatives, the system in normal form,

$$\begin{aligned} \dot{\xi}_1 &= -\xi_2 \\ \dot{\xi}_2 &= -\omega V\sqrt{1-\left(\tfrac{\xi_2}{V}\right)^2} \\ \dot{\eta} &= V\sqrt{1-\left(\tfrac{\xi_2}{V}\right)^2} \end{aligned} \tag{4}$$

$\xi_1 = d_{\text{center}}(x) - d_0$, $\xi_2 = \dot{d}_{\text{center}}(x)$, $\eta = -x\sin\gamma + y\cos\gamma$, has relative degree 2. Choosing the control

$$\omega = \frac{u}{V\sin(\gamma - \theta)} \tag{5}$$

with external input $u = -k_1\xi_1 - k_2\xi_2$, $k_1, k_2 > 0$, results in error dynamics $\dot{\xi}$ with stable poles

$$0 = s^2 + k_2 s + k_1 \tag{6}$$

and zero dynamics $\dot{\eta} = V$. The internal dynamics represent the movement in a direction parallel to the wall, and hence will not converge to 0 since the wheelchair is traveling at a constant speed V. While (1) is non-minimum phase due to the choice of output function, the error dynamics are by construction locally asymptotically stable under controller (5) for $d(x)$ in the neighborhood of d_0. The wheelchair can track a desired distance d_0 for $\theta \neq \gamma$, that is, for orientations other than ones for which the wheelchair is facing exactly towards or away from the wall. We choose $k_1 = 0.1$, $k_2 = 0.5$, the steady-state controller values obtained through LQR design with $Q = I, R = 100$, to penalize large inputs.

B. Turning around a corner

We transform (1) into polar coordinates with origin (p_x, p_y) corresponding to the corner, as shown in Figure 2,

$$\begin{aligned} r &\triangleq \sqrt{(x-p_x)^2 + (y-p_y)^2} \\ \phi &\triangleq \tan^{-1}\left(\tfrac{y-p_y}{x-p_x}\right) \end{aligned} \tag{7}$$

resulting in the dynamical system

$$\begin{aligned} \dot{r} &= V\cos(\phi - \theta) \\ \dot{\phi} &= -\tfrac{V}{r}\sin(\phi - \theta) \\ \dot{\theta} &= \omega \end{aligned} \tag{8}$$

To accomplish a constant radius turn, we choose output $r - r_0$ and again use input-output linearization. The system (8) has relative degree 2, and with $\xi_1 = r - r_0$, $\xi_2 = \dot{r}$, $\eta = \phi$,

$$\begin{aligned} \dot{\xi}_1 &= \xi_2 \\ \dot{\xi}_2 &= V\sqrt{1-(\tfrac{\xi_2}{V})^2}\left(\tfrac{V}{r}\sqrt{1-(\tfrac{\xi_2}{V})^2} + \omega\right) \\ \dot{\eta} &= -\tfrac{V}{\xi_1 + r_0}\sqrt{1-(\tfrac{\xi_2}{V})^2} \end{aligned} \tag{9}$$

The controller

$$\omega = -\frac{V\sin(\phi - \theta)}{r} + u \cdot \frac{1}{V\sin(\phi - \theta)} \tag{10}$$

with external input $u = -k_1\xi_1 - k_2\xi_2$, $k_1 > 0$, $k_2 > 0$ locally asymptotically stabilizes the error dynamics $\dot{\xi}$ for r within a neighborhood of r_0. As in the wall following maneuver, the system is non-minimum phase with zero dynamics $\dot{\eta} = -\frac{V}{r_0}$ representing a constant turn rate. In this mode, we choose $k_1 = 0.3$, $k_2 = 0.9$ via LQR with $Q = I$, $R = 10$.

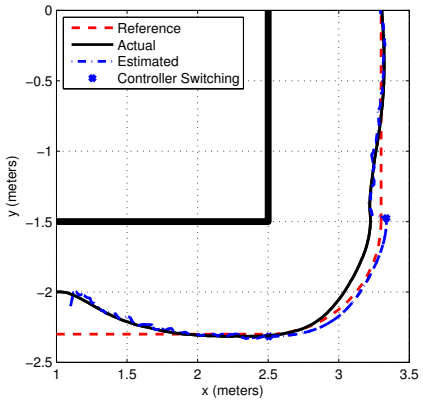

Fig. 3. Autonomous wall following around a corner. The trajectory begins in the lower left corner, and ends at the top right corner. Switching between wall following and turning is indicated by '*'.

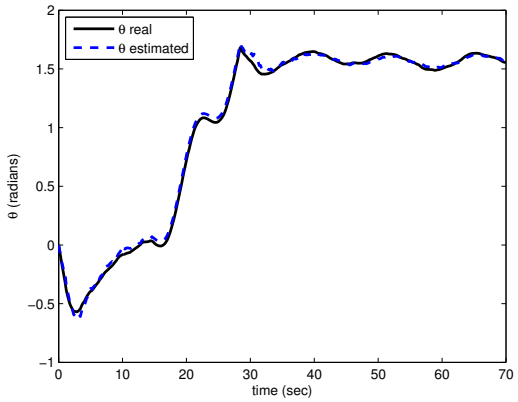

Fig. 4. Actual and estimated values of θ, from the indoor metrology ground-truth data, and from the extended Kalman filter, respectively.

C. Estimation

The controllers for wall following and turning around a corner require full knowledge of the state vector, however only limited information is available through the sensors: IR and wheel encoders. IR cannot be used for controlling a turn around a corner because of its inability to detect corners. Hence the turning maneuver uses only wheel encoders as inertial sensors, and hence is subject to integration errors. However, the wall following maneuver uses feedback from IR sensor measurements in addition to wheel encoders. The IR measurements are incorporated through the use of a discrete-time extended Kalman filter which determines an estimate $\hat{x}_k$ of the state at time $t_k = k\Delta$, $\Delta = 0.1s$ (10Hz sampling rate).

Consider (1) discretized [20] with IID Gaussian measurement and process noise (model uncertainty and wheel slip),

$$\begin{array}{rcl} \hat{x}_k & = & f(\hat{x}_{k-1}, u_k) + w_{k-1} \\ z_k & = & h(\hat{x}_k) + v_k \end{array} \tag{11}$$

with $\mathrm{Var}(w_k) = Q_k$, $\mathrm{Var}(v_k) = R_k$, and

$$\begin{array}{rcl} f(\hat{x}_{k-1}, u_k) & = & \begin{bmatrix} x_{k-1} + \Delta \cdot V_k \cos(\theta_{k-1} + \frac{1}{2}\omega_k \cdot \Delta) \\ y_{k-1} + \Delta \cdot V_k \sin(\theta_{k-1} + \frac{1}{2}\omega_k \cdot \Delta) \\ \theta_{k-1} + \omega_k \cdot \Delta \end{bmatrix} \\ h(\hat{x}_k) & = & d_{\mathrm{IR}}(\hat{x}_k). \end{array} \tag{12}$$

With values from [20], let $Q_{k-1} = \mathrm{diag}(Q_{11}, Q_{22}, Q_{33})$, with $Q_{11} = K_{ss}|V_k \cos\theta_{k-1}|$, $Q_{22} = K_{ss}|V_k \sin\theta_{k-1}|$, $Q_{33} = K_{s\theta}|V_k| + K_{\theta\theta}|\omega_k|$, and drift coefficients $K_{ss} = 0.001$, $K_{s\theta} = 0.0003$, $K_{\theta\theta} = 0.001$. Note that $R_k = \mathcal{N}(0, \sigma^2)$ depends on IR sensor properties; σ varies nonlinearly as a function of true distance to an object, with a maximum value $\sigma(80\mathrm{cm}) \leq 5\mathrm{cm}$.

The estimate is calculated through standard update and prediction steps [21]

$$\begin{array}{rcl} \hat{x}_{k|k-1} & = & f(\hat{x}_{k-1|k-1}, u_{k-1}) \\ P_{k|k-1} & = & A_k P_{k-1|k-1} A_k^T + Q_{k-1} \\ K_k & = & P_{k|k-1} H_k (H_k^T + P_{k|k-1} H_k + R_k)^{-1} \\ \hat{x}_{k|k} & = & \hat{x}_{k|k-1} + K_k(z_k - h(\hat{x}_{k|k-1})) \\ P_k & = & (I - K_k H_k^T) P_{k|k-1} \end{array} \tag{13}$$

with time-varying matrices

$$A_k = \frac{\partial f}{\partial x} \mid_{x=\hat{x}_{k-1|k-1}} = \begin{bmatrix} 1 & 0 & -\Delta \cdot V_k \sin\alpha_k \\ 0 & 1 & \Delta \cdot V_k \cos\alpha_k \\ 0 & 0 & 1 \end{bmatrix}, \tag{14}$$

$\alpha_k = \hat{\theta}_{k-1|k-1} + \Delta \cdot \frac{1}{2}\omega_k$, and $H_k = \frac{\partial h}{\partial x}^T \mid_{x=\hat{x}_{k|k-1}}$,

$$\frac{\partial h}{\partial x} = \frac{1}{\cos(\alpha_s - \gamma)} \begin{bmatrix} \cos\gamma \\ \sin\gamma \\ \beta(x) + d_{\mathrm{IR}}(x)\sin(\alpha_s - \gamma) \end{bmatrix}, \tag{15}$$

with $\beta(x) = -x_s' \sin(\theta - \gamma) + y_s' \cos(\theta - \gamma)$, and initial conditions $P_{0|0} = \mathrm{Var}(x_0)$, $\hat{x}_{0|0} = E[x(0)]$.

Hence the controllers (5) and (10) will use the most current state estimate in lieu of the actual state x. Details regarding implementation in ROS are described in [22].

EXPERIMENTAL RESULTS

The wall following and turning maneuvers were combined to guide the wheelchair autonomously following one wall, turning around a corner, then continuing to follow the wall in a new direction. An indoor metrology system (Metris Inc., iGPS System) provides external validation of the actual trajectory of the wheelchair with sub-millimeter accuracy.

Figures 3 and 4 show planar motion and heading of the wheelchair, respectively. The initial distance is ≈0.25m from d_0, yet the wheelchair quickly corrects itself within 1m of travel. The location of the corner is hard-coded via the encoders to trigger switching from wall-following to turning around the corner, and switching back to wall-following at the end of the corner, since our current focus is on the continuous controller and its noise rejection capabilities. Despite the heterogeneity in IR measurements (e.g., "range") in Figure 5, the wheelchair maintains a fairly precise path. The sharp transition from non-zero values to a zero range indicates the lack of measurable signal as the wheelchair rounds the corner, and the wall falls out of the range of view of the IR sensor.

The control authority required to complete this series of maneuvers is shown in Figure 6. Saturation is not an issue

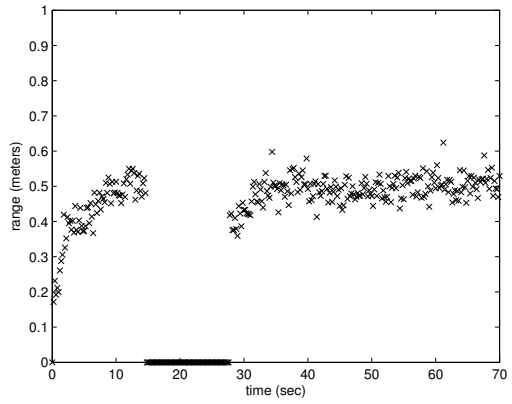

Fig. 5. IR sensor readings for the trajectory shown in Figure 3. When the wall is no longer within the range of the IR sensor as the wheelchair reaches the corner, the IR sensors return a 0 range value.

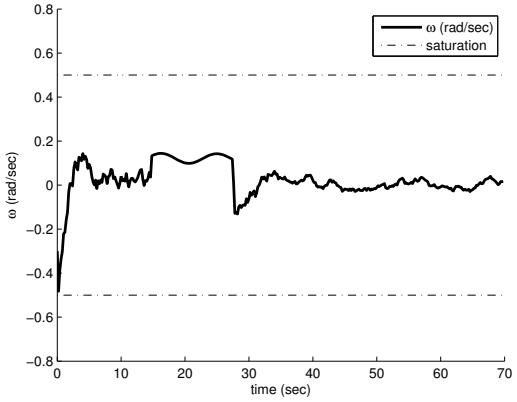

Fig. 6. Input history for the trajectory shown in Figure 3. The sharp changes correspond to a switch from wall following to turning, and back to wall following.

due to the choice of pole locations, indicating that higher performance is possible.

CONCLUSIONS

We described a mathematical model and controller design for autonomous wall following around a corner based on IR and wheel encoder measurements. We experimentally validated our results on a smart wheelchair platform at UBC. In the future, we plan to demonstrate additional Wheelchair Skills Test functionalities autonomously, including more robust switching schemes and different sensor modalities, with the ultimate goal of developing a collaborative smart wheelchair.

ACKNOWLEDGMENTS

This work is funded by NSERC Discovery Grant #298211 (Mitchell), NSERC Discovery Grant #387327 (Oishi), CFI Leaders Opportunity Fund / BC KDF #13113 (Oishi), CIHR Team in Wheeled Mobility for Older Adults (W. Miller), and an NSERC USRA (Cheng). We thank Richard Yu, Timothy Tang, Sean Ding, and Amy Leson for their assistance.

REFERENCES

[1] R. Cooper, "Quality-of-life technology," *IEEE Engineering in Medicine and Biology*, vol. 27, pp. 10–11, March/April 2008.

[2] D. Ding and R. Cooper, "Electric-powered wheelchairs: A review of current technology and insight into future directions," *IEEE Control Systems Magazine*, vol. 25, pp. 22–34, April 2005.

[3] P. Viswanathan, J. Boger, J. Hoey, P. Elinas, and A. Mihailidis, "The future of wheelchairs: Intelligent collision avoidance and navigation assistance," *Geriatrics and Aging*, vol. 10, no. 4, pp. 253–256, 2007.

[4] "Advancing the inclusion of people with disabilities," Tech. Rep. SD23-4/2005E, Government of Canada, Canada, 2005.

[5] W. Mortenson, W. Miller, J. Boily, B. Steele, E. Crawford, and G. Desharnais, "Overarching principles and salient findings for including in guidelines for power mobility use within residential care facilities," *Journal of Rehabilitation Research and Development*, vol. 43, pp. 199–208, March 2006.

[6] R. Simpson, "Smart wheelchairs: A literature review," *Journal of Rehabilitation Research and Development*, vol. 42, pp. 423–436, July 2005.

[7] A. Mihailidis, P. Elinas, J. Boger, and J. Hoey, "An intelligent powered wheelchair to enable mobility of cognitively impaired older adults: An anticollision system," *IEEE Transactions on Neural Systems and Rehabilitation Engineering*, vol. 15, pp. 136–143, March 2007.

[8] R. Simpson, E. LoPresti, S. Hayashi, S. Guo, D. Ding, W. Ammer, V. Sharma, and R. Cooper, "A prototype power assist wheelchair that provides for obstacle detection and avoidance for those with visual impairments," *Journal of NeuroEngineering and Rehabilitation*, vol. 2, p. 30, October 2005.

[9] R. H. Wang, S. M. Gorski, P. J. Holliday, and G. R. Fernie, "Evaluation of a contact sensor skirt for an anti-collision power wheelchair for older adult nursing home residents with dementia: Safety and mobility," *Assistive Technology*, 2010. In press.

[10] P. Viswanathan, A. Mackworth, J. J. Little, J. Hoey, and A. Mihailidis, "NOAH for wheelchair users with cognitive impairment: Navigation and obstacle avoidance help," in *Proceedings of AAAI Fall Symposium on AI in Eldercare: New Solutions to Old Problems*, (Washington, DC), pp. 150–152, 2008.

[11] R. Simpson and S. Levine, "Voice control of a powered wheelchair," *IEEE Transactions on Neural Systems and Rehabilitation Engineering*, vol. 10, pp. 122–125, June 2002.

[12] S. Parikh, V. Grassi, V. Kumar, and J. Okamoto, "Integrating human inputs with autonomous behaviors on an intelligent wheelchair platform," *IEEE Intelligent Systems*, vol. 22, pp. 33–41, March/April 2007.

[13] T. Carlson and Y. Demiris, "Human-wheelchair collaboration through prediction of intention and adaptive assistance," in *Proceedings of the IEEE International Conference on Robotics and Automation*, (Pasadena, CA), pp. 3926–3931, 2008.

[14] A. Atrash, R. Kaplow, J. Villemure, R. West, H. Yamani, and J. Pineau, "Development and validation of a robust speech interface for improved human-robot interaction," *International Journal of Social Robotics*, vol. 1, no. 4, pp. 345–356, 2009.

[15] P. van Turennout, G. Honderd, and L. van Schelven, "Wall-following control of a mobile robot," in *IEEE International Conference on Robotics and Automation*, vol. 1, pp. 280–285, May 1992.

[16] A. Bemporad, M. Di Marco, and A. Tesi, "Wall-following controllers for sonar-based mobile robots," in *Proceedings of the IEEE Conference on Decision and Control*, vol. 3, pp. 3063–3068, 1997.

[17] Willow Garage, "Ros.org." Website, 2010. http://www.ros.org/wiki.

[18] C. Smith and R. Kirby, "Wheelchair Skills Test as a means of assessing power mobility," in *Proceedings of the Canadian Seating and Mobility Conference*, (Toronto, ON), p. 130, September 2001.

[19] G. Campion, G. Bastin, and B. Dandrea-Nove, "Structural properties and classification of kinematic and dynamic models of wheeled mobile robots," *IEEE Transactions on Robotics and Automation*, vol. 12, no. 1, pp. 47–62, 1996.

[20] F. Chenavier and J. Crowley, "Position estimation for a mobile robot using vision and odometry," in *Proceedings of the IEEE International Conference on Robotics and Automation*, May 1992.

[21] R. Stengel, *Optimal Control*. Berlin, Germany: Springer-Verlag, 1995.

[22] M. Oishi, A. Cheng, P. Taghipour Bibalan, and I. Mitchell, "Buildling a smart wheelchair on a flexible software platform," in *RESNA Annual Conference*, 2011. Submitted.